OUTGASSING RATE OF MULTILAYER INSULATION

A. P. M. Glassford and C. K. Liu
Lockheed Palo Alto Research Laboratory

1.0 INTRODUCTION

Multilayer insulation (MLI) is used extensively in space systems in applications where high thermal resistance plus very light weight are required, such as the insulation of cryogenic systems, and a variety of critical external surfaces such as the back side of radiators. MLI consists of many thermal radiation shields arranged in series, usually interleaved with a low conductance spacer material to reduce thermal conduction between shields. To achieve maximum thermal resistance a great many shields in series are required, and consequently the shields and spacers are made of very lightweight materials so as to avoid excessive weight. Shields are customarily made by vacuum depositing a 500-1000 Å layer of gold or aluminum on one or both sides of Mylar or Kapton substrates with nominal thickness in the range 0.25 - 2.0 mils. The actual thickness of the metal film is adjusted to obtain the desired low emittance value for low radiation heat transfer. Commonly used spacing materials include netting made from silk, nylon or Dacron, or very thin glass fibers, such as 'Tissuglas' and 'Dexiglas' cloths.

Since MLI materials are very light weight, the total mass of MLI is relatively small in most applications. On the other hand, because of the many layers required the total surface area can be extremely high, making MLI a significant outgas source, and, because the surface to volume ratio is high, the major outgas product is water vapor. MLI outgassing can affect overall system performance in two principal ways. Firstly, outgassing products can degrade the performance of the MLI

system itself by raising the gas pressure between the shields sufficiently for gaseous conduction to become significant. Insulation degradation can also occur if sections of the MLI are cold enough to cause condensation of outgas products, which will raise the emissivity of the shields and increase the radiation heat transfer. Secondly, as an outgassing source MLI can degrade the performance of associated systems. MLI outgassing can delay the attainment of low pressures in test chambers and vacuum enclosures, while on the ground and in orbit outgas products can condense on optical and thermal control surfaces. This latter situation is probably the most critical current MLI-caused problem area, because of the increasing use of cryogenic sensor systems. Outgassed water vapor can also contribute to the contaminant cloud surrounding an orbiting spacecraft.

In order to minimize or eliminate problems introduced by MLI outgassing, careful design studies must be made for which an outgassing data base is required. The type of data needed for such analyses are outgassing rates per unit area as a function of time for the various temperature histories of specific interest for all materials of interest. However, temperature history can take an infinite variety of forms, so it is impossible in practice to obtain sufficient data to represent all situations. A more practical approach is to obtain isothermal outgassing rate data at various specific temperatures, and then to estimate the rates for other constant or varying temperature situations by use of analytical models. The work reported in this paper is directed towards this end. Isothermal outgassing rate data have been obtained for a range of temperatures for a selection of commonly-used MLI shields and spacers. An attempt has been made to incorporate the data into various previously-proposed analytical models. The reported work is part of an Independent Research program in progress at Lockheed and further data and analyses of the type described will become available from this program in the near future.

MLI outgassing rates have been measured as a function of time in previous programs.[1], [2], [3] These previous measurements were all based upon pressure measurements. This limited the available sensitivity of the measurement, and depended, in principle, on the assumption that the outgas products would not be adsorbed on the apparatus walls. These limitations were aggravated when measurements at temperatures other than ambient were made. In the present tests a technique based on collection of the outgas species on a cooled quartz crystal microbalance (QCM) was used. The technique permits between one and three orders of magnitude better sensitivity and accuracy to be achieved, while variable sample temperature operation presents no additional problem.

2.0 EXPERIMENTAL PROGRAM

2.1 Sample Material

The types and specifications of the materials tested to date are listed in Table 1. Additional shield materials will be tested, including Mylar with a single coat of both aluminum and gold, Kapton with various types of coating and 'Dexiglas' glass fiber cloth.

2.2 Test Schedule

The test schedule to date is shown in Table 2. The range of test temperatures selected for each material includes the ambient temperature of 25°C; a maximum temperature of about 125°C; the lowest temperature for which the outgassing rate is measurable; and as many isotherms

1. Keller, C. W., High Performance Thermal Protection Systems," Rept. LMSC A-964947, Dec. 1969, Lockheed Missiles & Space Company, Sunnyvale, California, pp 4.1-4.26.
2. Glassford, A. P. M., Outgassing Behavior of Multilayer Insulation Materials, J. Spacecraft and Rockets, Vol. 7, No. 12, Dec. 1970, pp. 1464-1468
3. Parmley, R. T., Smith, F. J., Glassford A. P. M., Coleman, J., and Stevenson, D. R., Effect of Environment on Insulation Materials - Vols. 1 and 2. NASA-CR 120978 and 120979 (1973), Final Report, Contract NAS 3-14342, Lockheed Missiles & Space Company, Inc.

between these limits are deemed necessary to establish the temperature variation of outgassing rate over this range. A complete set of isotherms has been obtained for double-aluminized Mylar and Dacron net. The remaining materials have been tested only at 25°C so far in order to complete a representative comparison of materials before this conference.

TABLE 1. MULTILAYER INSULATION MATERIAL SPECIFICATIONS

MATERIAL	NOMINAL DIMENSIONS	MANUFACTURER'S NAME/STYLE
Double-aluminized Mylar	-0.25 mils thick	National Metallizing Div.,
Double-goldized Mylar	-500 to 1000Å metal film -8.7×10^{-4} gm/cm^2 (Al) -1.1×10^{-3} gm/cm^2 (Au)	Standard Pack. Corp., Cranbury, N. J. 08512
Dacron Net	-8.7 hex. meshes/cm^2 -6.7 mils thick -6×10^{-4} gm/cm^2	Apex Mills 49 W. 37th Street New York, N. Y. 10018 - Style B-4A
Nylon net	$-13\frac{1}{4}$ hex. meshes/cm^2 -9 mils thick -1.4×10^{-3} gm/cm^2	Sears Roebuck (any store)
Silk Net	-32.5 hex. meshes/cm^2 -5 mils thick -6×10^{-4} gm/cm^2	John Heathcoat Company 108 W. 39th Street New York, N. Y. 10018 Silk Illusion Net
Tissuglas (Glass Fiber Paper)	-0.6 mils thick -4.2×10^{-4} gm/cm^2	Pallflex Prod. Corp. Kennedy Drive Putnam, Conn. 06260 - Style 60G

TABLE 2 - TEST SCHEDULE

Material	Nominal Samples Area - In^2	Test Temperatures - ^oC
Double-Aluminized Mylar	~1600	-54; -34; -8; 25; 50; 81; 121
Double-Goldized Mylar	1728	25
Dacron Net	~3000	2.5; 12/5; 25; 57.2; 126
Silk Net	1536	25
Nylon Net	1903	25
Tissuglas	3056	25

The duration of each isothermal test was one week. This period represented a balance between obtaining adequate long term data, and completing the test program in a reasonable time. One week permits a convenient practical turn-around schedule, while the data for this period can be reliably extrapolated to several weeks duration.

2.3 Apparatus Description

The experimental outgassing rate measurements were made by using the Thermal Analysis Apparatus (TAA), shown in Figure 1. The principal components of the TAA are a sample pot, a collector QCM, and a system of shrouds which are thermally grounded to a liquid nitrogen reservoir. The sample pot is a cylindrical container with a small orifice in one end. Its base contains an electrical resistance heater and a platinum resistance thermometer. It is supported by a strut attached to the cooled shrouding, which serves as a thermal link. The sample pot temperature can be controlled to any value above 120^oK by balancing the electrical heat input to the pot against the heat leak along the strut to the shrouds.

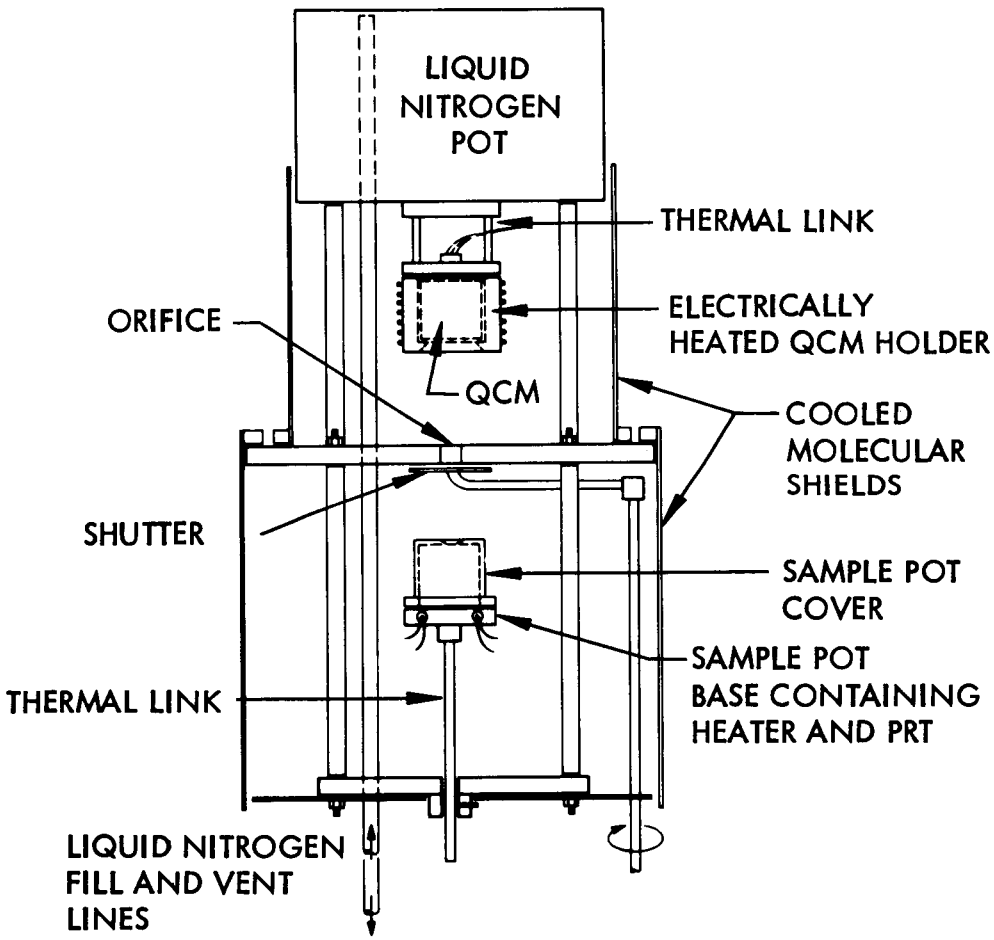

FIGURE 1 - SCHEMATIC OF THERMAL ANALYSIS APPARATUS

The collector QCM, mounted in an aluminum holder with an electric resistance heater, is positioned along the normal line of sight of the sample pot orifice. The QCM views the sample pot orifice through a shuttered hole in the shielding structure, permitting the impinging flux to be interrupted when appropriate. The QCM normally cools naturally to about $84^{\circ}K$, at which temperature all significant outgas species impinging on its surface will be condensed. However, its temperature can be controlled to any temperature between $84^{\circ}K$ and $420^{\circ}K$ by balancing electrical heat input against heat leakage along its support struts to the liquid nitrogen reservoir. The QCM is a Celesco Model 700 unit, which contains a built-in platinum resistance thermometer. The accuracy of this QCM has been established in a previous work.[4] The apparatus shown in Figure 1 is enclosed in a bell jar which can be evacuated to a pressure less than 2×10^{-7} torr. The fundamental data output from the apparatus are QCM frequency and temperature, and sample pot temperature. These data are recorded continuously as a function of time by automatic instrumentation.

2.4 Experimental Procedure

At the beginning of the test the area of the sample material is measured, and the sample is inserted in the sample holder. The sample holder is assembled with the apparatus, and the distance between the sample pot orifice and the QCM surface is measured. The bell jar is then evacuated and the apparatus cooled by filling the liquid nitrogen pot. Evacuation to 10^{-5} torr takes about 3 minutes, while cooldown of the QCM to its equilibrium temperature of $84^{\circ}K$ and attainment of 2×10^{-7} torr takes about 40-60 minutes. As soon as the apparatus has been evacuated the sample pot temperature is adjusted to a selected constant temperature value. Above-ambient temperatures can be reached in less than one-half

4. Glassford, A. P. M., Analysis of the Accuracy of a Commercial Quartz Microbalance, Progress in Astronautics and Aeronautics, Volume 56, Allie M. Smith, Ed., American Institute of Aeronautics and Astronautics, New York, (1977).

hour by heating the pot rapidly, followed by adjustment of the electric power to the equilibrium value. For subambient temperatures the pot cools naturally with the main apparatus, reaching temperatures of the order of -50°C in two hours. The experiment consists of collecting the outgas product from the sample pot by condensation on the cold QCM. Collection begins as soon as the QCM has cooled below the temperature at which the outgas products can condense. The main outgas product from most MLI materials is water vapor, which condenses in vacuum at temperatures below about 155°K. This temperature is reached about 25 minutes after beginning the test. Outgas products are collected for one week, during which time sample pot temperature control, liquid nitrogen pot refilling and data recording are performed automatically. At the end of the test period data recording is terminated, electric power inputs switched off, and the apparatus allowed to warm up.

From time to time during a test, as well as at the end of the test period, the QCM was warmed up in a controlled manner, to determine the evaporation characteristics of the accumulated deposit. This involves heating the QCM at about 1-2°K per minute and recording the QCM frequency and temperatures as a function of time.

2.5 Data Reduction

It is assumed that all the molecular flux striking the 84°K collector QCM is condensed. This assumption is correct for H_2O, which is the principal component, and almost certainly possesses the lowest molecular weight among the outgassed species. The error introduced by equating the molecular flux collected by the QCM to the absolute flux striking it is therefore considered to be negligible. The molecular flux impinging on the QCM is therefore given by

$$\left(\frac{\dot{m}}{A}\right)_Q = \frac{df}{dt} \times S \text{ gms/cm}^2/\text{sec}$$

where f is the QCM frequency, and S is the QCM sensitivity constant (4.43×10^{-9} gm/cm^2/Hz for the Celesco Model 70QA QCM). The mass flux at the QCM surface is related to the total mass leaving the sample pot orifice, $\dot{m}_o$, by a view factor. For an infinitely thin orifice the distribution of flux leaving it should be cosine. The effect of finite orifice thickness is to reduce the flux at large angles and increase it along the normal. The magnitude of this effect has been measured in a previous test, and is allowed for by introducing a factor of 0.98 in the equation relating $\dot{m}_o$ to $(\dot{m}/A)_Q$. Thus

$$\dot{m}_o = \frac{\dot{m}}{A}_Q \times (0.98 \pi r^2)$$

where r is the distance from the sample pot orifice to the QCM surface. The outgassing rate of the sample, $\dot{Q}$, is found by dividing $\dot{m}_o$ by the sample area. The area used is the total exposed area, which is twice the nominal area.

$$\dot{Q} = \dot{m}_o/(2 \times \text{nominal sample area})$$

All data are recorded from the beginning of evacuation and plotted against time elapsed since this event. The evacuation times given in this paper thus include the time required to adjust the sample temperature to the selected equilibrium value. Although this time can range from zero, for the 25°C sample, up to 2 hours for temperatures below -50°C the average time required for equilibrium was less than one-half hour.

The frequency/time data obtained during QCM warm-up are related to the evaporation rate of the collected deposit, $(\dot{m}_e/A)$, as follows

$$\frac{\dot{m}_e}{A} = - \frac{df}{dt} \times \frac{(4.43 \times 10^{-9})}{0.81}$$

The factor 0.81 is introduced in this equation to allow for the flow resistance of the aperture in its case through which the QCM crystal views the exterior.[4]

2.6 Experimental Data

The results of the experiments conducted to date are discussed below in three main groups - measurements at 25°C on several materials, and measurements for a comprehensive range of temperatures on both double-aluminized Mylar and Dacron net. In all cases, the data consist of measurements of outgassing rate versus time for a period of 6 to 7 days. At the end of this period the QCM was slowly heated to identify the collected components by their reevaporation characteristics. In all cases, the principal outgas component was H_2O, identified by its evaporation characteristics. The evaporation of water from a QCM of this type has been studied in some detail previously[4] and so H_2O can be identified with some certainty. In most tests no species but water could be detected. Since the sensitivity of this test is about 0.5 per cent it is concluded that in most cases at least 99.5 per cent of the outgas species collected under the specified test conditions was H_2O. The single exception to this conclusions -- Dacron net tested at above ambient temperatures -- is discussed in Section 2.6.3.

2.6.1 Ambient Temperature Data

Figure 2 shows outgassing rate versus time for several materials at 25°C. It is apparent that Dacron net has a significantly lower outgassing rate than either silk or Nylon net, and is clearly the preferred net, based upon outgassing considerations. The data for the three nets suggest that detailed studies of the variation of the outgassing rate of silk and Nylon net with temperature would serve little practical purpose. Tissuglas is a commonly used spacer, and has been used in several flight systems by Lockheed. It is generally used in MLI systems having a higher

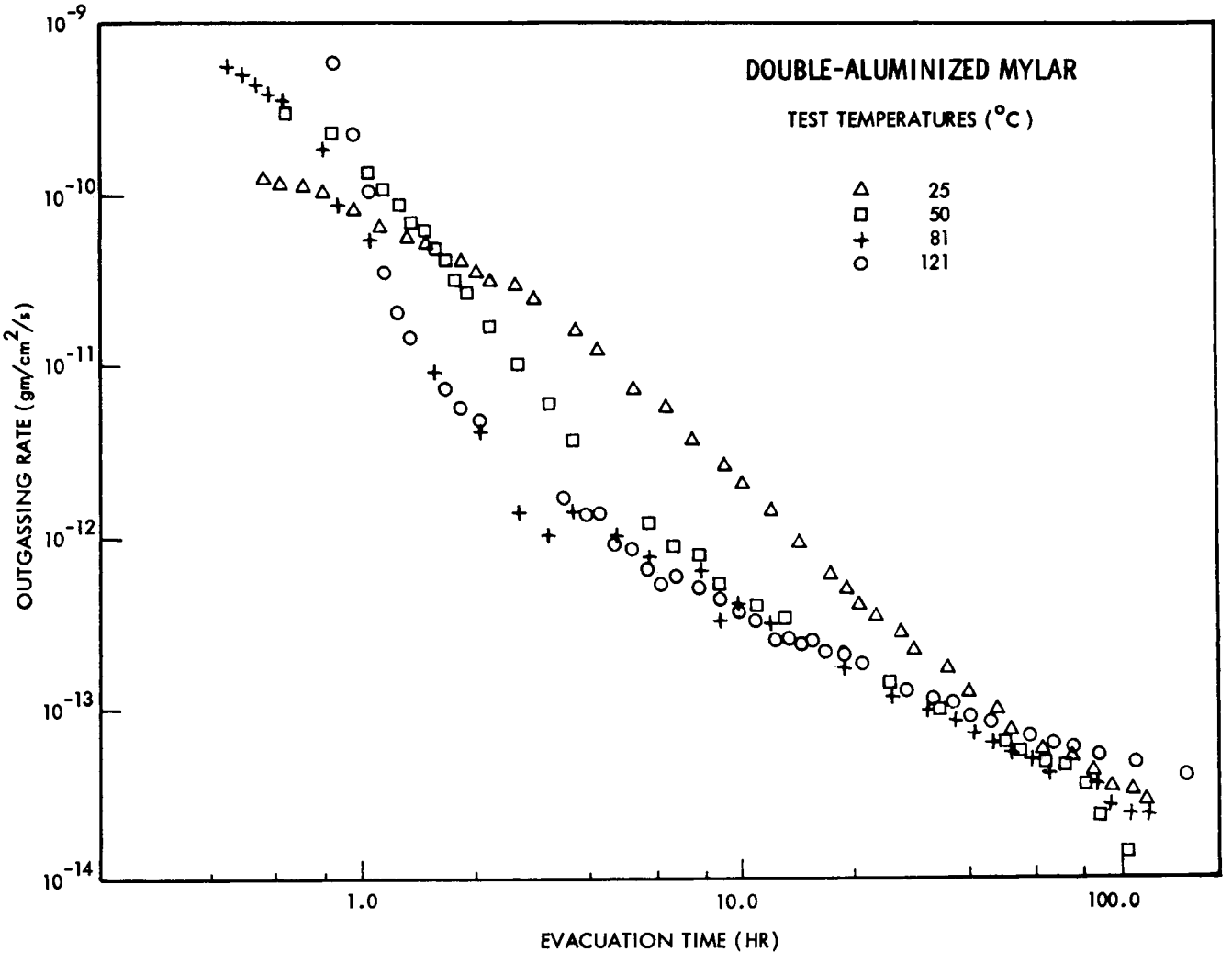

FIGURE 2 - OUTGASSING RATE AT 25°C FOR VARIOUS MULTI-LAYER INSULATION MATERIALS

total number of layers than systems which use net spacers. The data therefore indicate that Tissuglas-spaced MLI will outgas between one and two orders of magnitude more than Dacron net-spaced MLI.

Comparison of the data for double-goldized and double-aluminized Mylar shows that they are basically similar in absolute value and in the shape of the curves. The single difference is that the slight 'knee' which appears in the aluminized Mylar data at about 3 hours is delayed until about $4\frac{1}{2}$ hours for the golidzed sample. A reasonable conclusion from these data is that the major amount of H_2O collected during the test originates in the material component common to both shields, i.e., the Mylar substrate, while the apparent delay could be due to the different permeabilities of the metallic films, or to a slight difference in the thicknesses of the Mylar substrates.

2.6.2 Double Aluminized Mylar

This material has been tested at seven temperatures. The lowest temperature selected was $-54^{\circ}C$, below which the outgassing rate is too small to be measured. The upper temperature, $121^{\circ}C$, was arbitrarily selected to be close to the temperature used in TML/VCM tests. Outgassing rate versus time is shown in Figure 3 for temperatures of $25^{\circ}C$ and above, and on Figure 4 for temperatures of $25^{\circ}C$ and below. The data have been separated in this manner to avoid visual confusion, and to assist in the description of the analytical modelling effort in Section 3. At the three lower temperatures it appears as if one outgassing mechanism predominates, which is gradually accelerated as the temperature is raised. When the temperature reaches $25^{\circ}C$, a second mechanism appears to become significant at times greater than about 14 hours. Further raising of the temperature accelerates the first mechanism still further until it is over within an hour, and several slower mechanisms now become predominant in the time period of interest. Further heating does not produce a reduction in the outgassing rate at long evacuation times, as would be expected if a limited number of

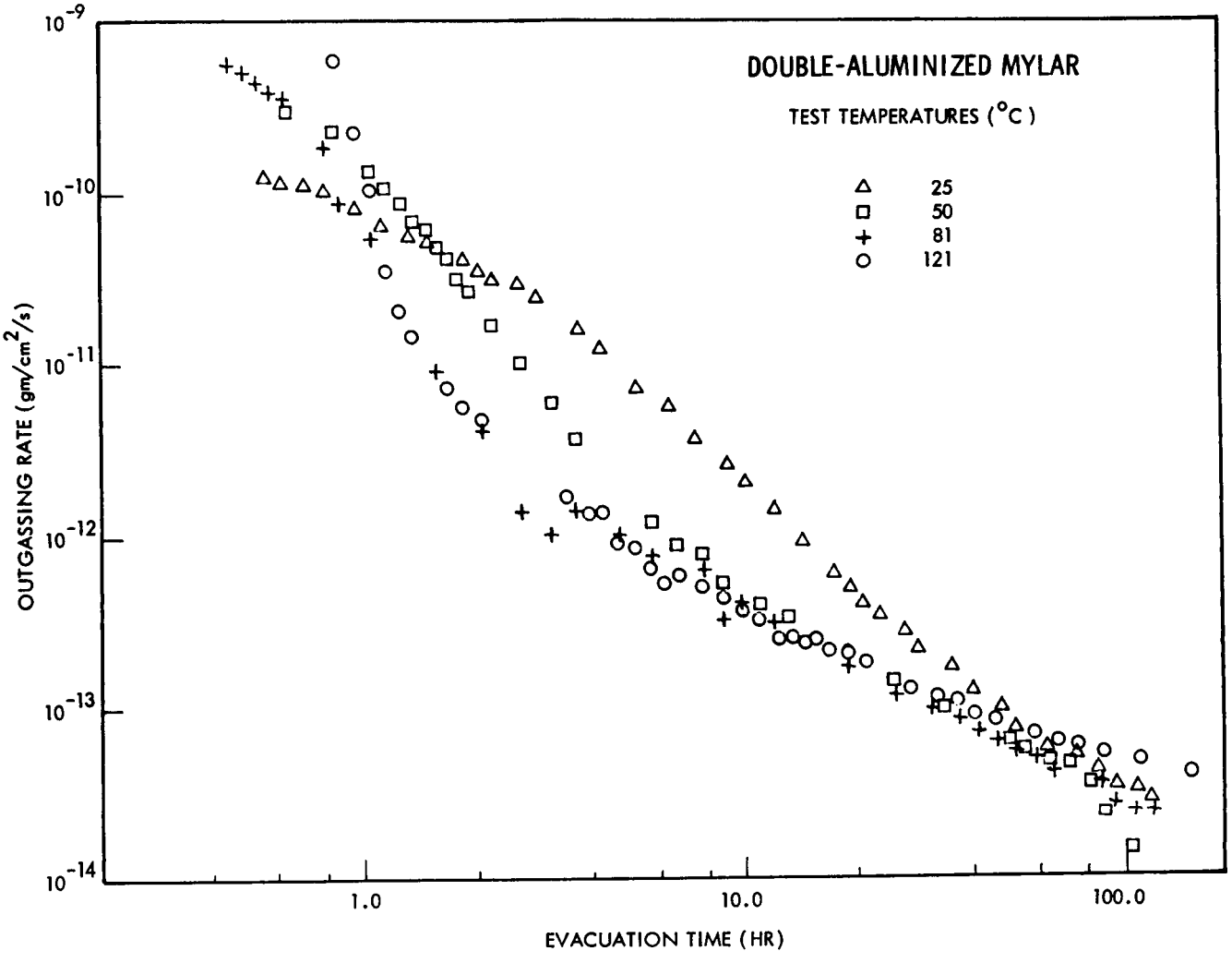

FIGURE 3 - OUTGASSING RATE OF DOUBLE-ALUMINIZED MYLAR FOR TEMPERATURES OF 25°C AND ABOVE

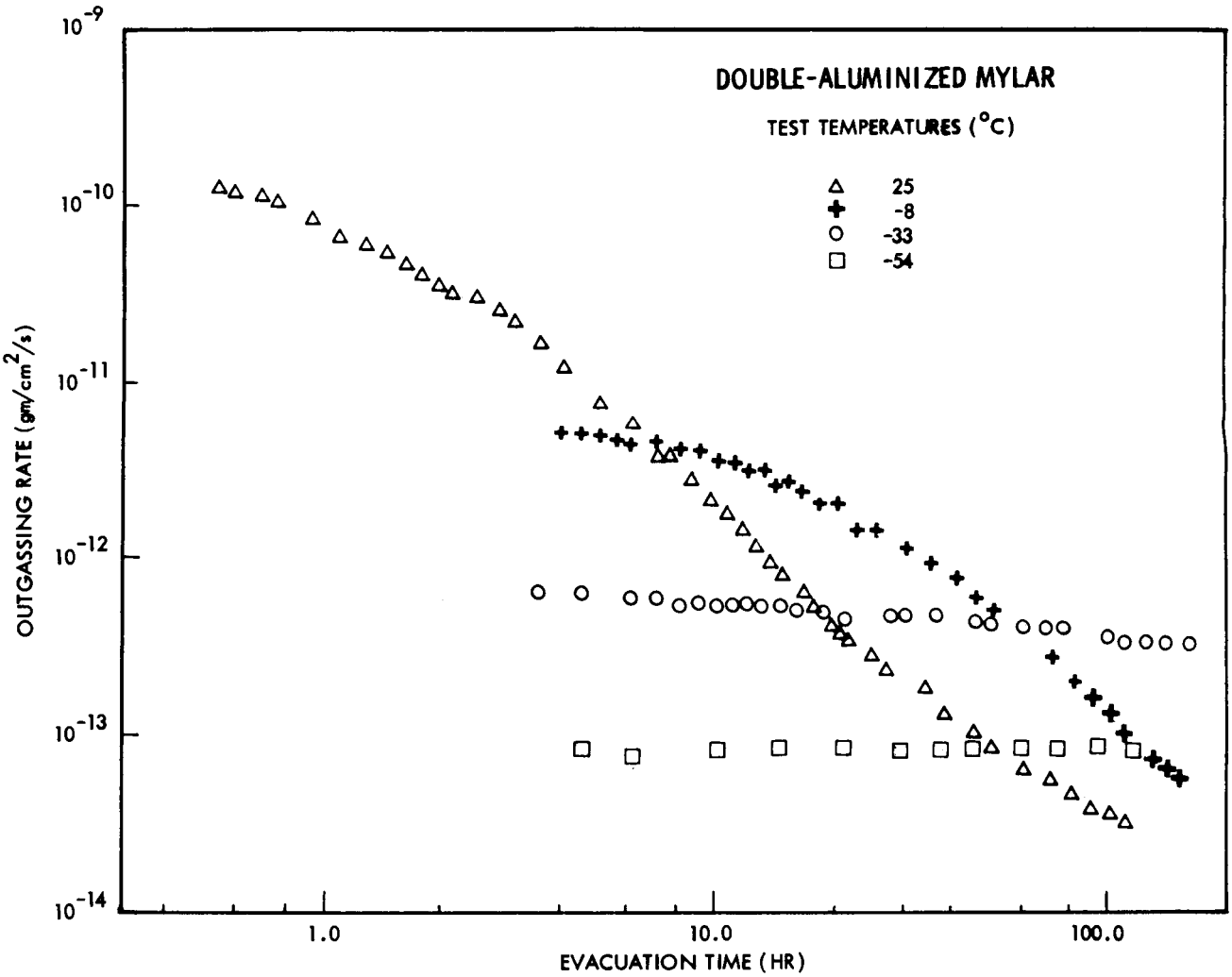

FIGURE 4 - OUTGASSING RATE OF DOUBLE-ALUMINIZED MYLAR FOR TEMPERATURES OF 25°C AND BELOW

mechanisms were present. Instead, the outgassing rates at times over 50 hours seem to vary little with increasing temperature, indicating the progressively increasing significance of previously minor outgas mechanisms with presumably higher activation energies.

Two short additional tests were conducted on double-aluminized Mylar to assess the effectiveness of bakeout on the outgassing rate. In these tests the samples were heated in vacuum to 45°C and 100°C, respectively, for 24 hours, after which they were cooled to 25°C, and their outgassing rates measured for another 24 hours. Preconditioning in this manner at 45°C and 100°C reduced the outgassing rate at 48 hours by factors of ten and two hundred, respectively, compared with the unpreconditioned 25°C data.

2.6.3 Dacron Net

This material has been tested at five temperatures. The maximum temperature range was selected according to the same criteria as were described in Section 2.6.2. The data are presented in Figure 5. For most of the temperature range the isotherms are displaced upwards as the temperature is increased. This slope, and the associated temperature dependence, is characteristic of diffusion in a heterogeneous system, i.e., system in which there could be variations in either diffusion flow path length or activation energy for diffusion, or both. The (-1) slope is obtained when the diffusion time constant, which can depend on flow path length and activation energy, and the amount of absorbed gas with a given time constant have an inverse linear relationship. At longer evacuation times or higher temperatures this type of relationship eventually produces an exponential relationship which is evident in the early portion of the 126°C data. The outgassing rate at later times for 126°C has a -1 slope, and is probably due to the onset of outgassing a different species. This conclusion is supported by QCM warm-up data which indicate that for tests at 25°C and below the outgas species is at least 99.5 per cent H_2O, in common with the other materials. At 57°C, however, other species appear in small amounts, while at 126°C

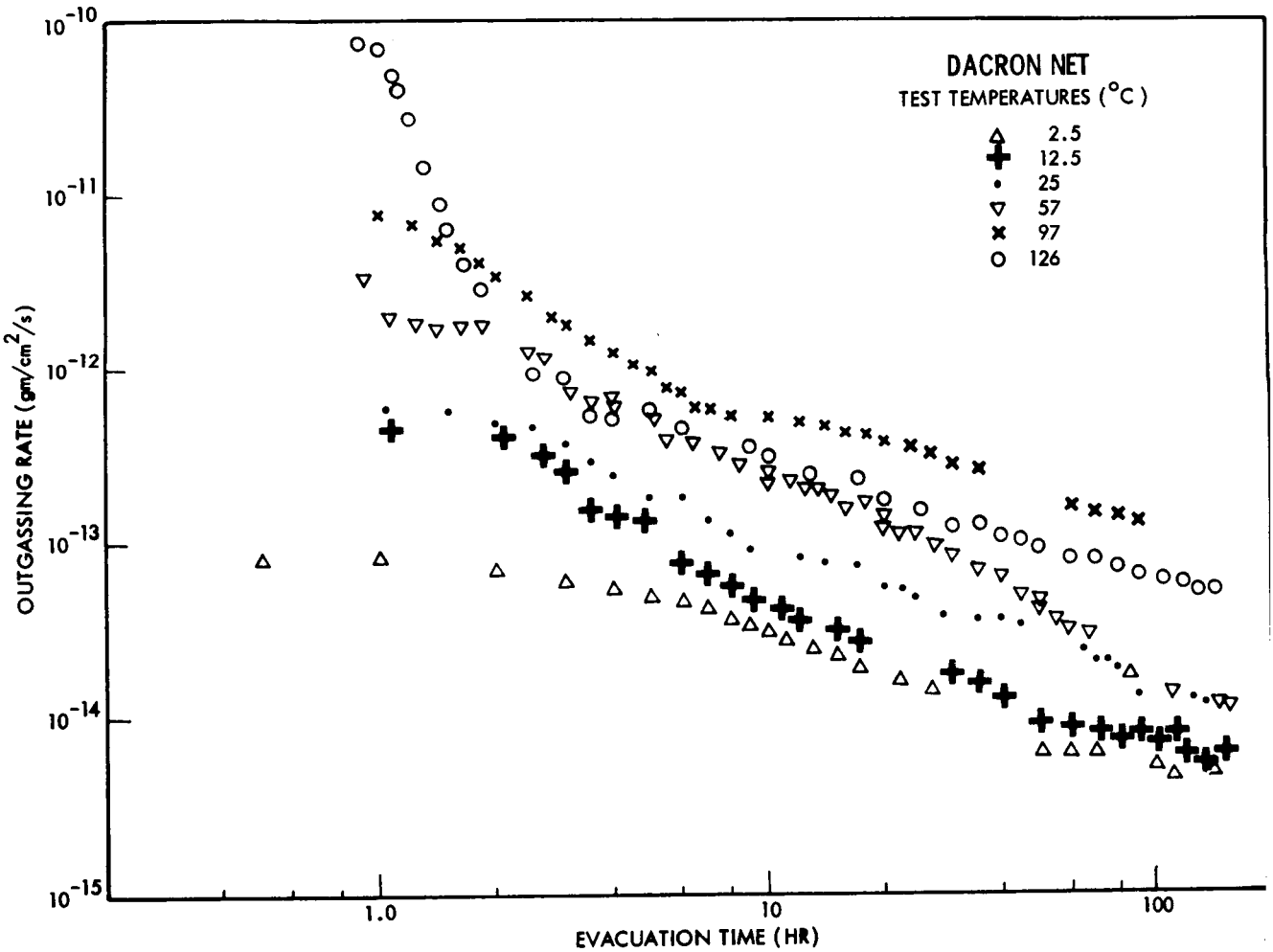

FIGURE 5 - OUTGASSING RATE OF DACRON NET FOR A RANGE OF TEMPERATURES

two distinct species other than H_2O were found in very significant proportions.

The QCM warm-up data indicate that at 126°C the proportions of H_2O and the two other species are approximately 54, 16 and 30 per cent respectively, in order of decreasing volatility. At 57°C the two less volatile species were difficult to separate by QCM warm-up, and amounted to less than 10 per cent of the total outgas product (the remaining 90 per cent being H_2O). For both isotherms the volatities of these two additional species were difficult to estimate accurately because of the small deposits obtained on the QCM. However, it is estimated that the 16 per cent component would be totally condensible at -90°C, and non-condensible on a -45°C surface. Similar figures for the 30 per cent component are 0°C and 40°C, respectively.

3.0 ANALYTICAL MODELLING

3.1 General Observations

Although analytical models based on time physical outgas-controlling mechanisms are unquestionably more desirable for predicting outgassing rate than empirical models, development of such models is probably impractical if the sole aim is to solve specific and immediate program problems. This is because it is necessary to generate a very large data base from which to develop the models, while these data may be more than sufficient themselves to satisfy the program need. Further, if analytical representations of the data are desired, it will be acceptable in many cases, as well as being simpler, to use empirical expressions instead of such models to represent the experimental data. However, insight into these outgas controlling mechanisms can only be obtained by developing expressions in terms of relevant physical parameters, and this is the ultimate goal of the present work.

The two main processes controlling outgassing are bulk diffusion and surface desorption. Theoretical expressions for these processes are readily available, but are difficult to apply to MLI materials. These

materials characteristically have very small dimensions from bulk center to surface, which tends to blur the distinction between bulk processes and surface processes. In the case of the nets and glass fiber papers normal variations in fiber diameter, and the micropore structure of their surfaces can be of the same order of magnitude as the nominal diameter itself. The same considerations apply to the Mylar and Kapton shield materials, but with the added influence of the metallic film. In the nominal thickness range of 500 Å to 1000 Å the film is not continuous, but is based on an island structure which grows into a film by bridging between islands. In the case of aluminum an oxide film is formed on this structure. The metallic film complicates the situation by providing an added diffusion resistance for material diffusing out from the interior of the substrate, while providing a complex microstructured surface for physical adsorption and possibly weak chemisorption in the oxide film. The net effect on both spacers and shields is to complicate the diffusion and desorption processes by introducing distributions of activation energies and characteristic dimensions.

3.2 Analysis of Double-Aluminized Mylar Data

A first attempt at analytical representations was made on data for double-aluminized Mylar. Figure 4 shows that for temperatures of 25°C and below, processes of longer time constants appear to have been suppressed sufficiently such that a single mechanism dominates outgassing for the -54°C and -34°C isotherms and for the early part of the -80°C and 25°C isotherms. This portion of the data was therefore selected for the initial analytical study.

3.2.1 Empirical Equation

Before attempting to develop a physical model the early data of Figure 4 were fitted empirically, as follows

$$\dot{Q} = \left((4.76 \times 10^{-7})/t_c \right) \exp(-t/t_c) \text{ gms/cm}^2\text{/sec} \qquad (1)$$

where

$$t_c = 2.8 \times 10^{-6} \exp(12600/RT) \text{ secs} \qquad (2)$$

This equation gives the outgassing rate of the subject data with an accuracy of about $\pm$ 25 per cent.

3.2.2 Physical Models

As noted in Section 3.1 the basic outgassing mechanisms of diffusion and desorption are confused in the case of MLI by the possibility of variable activation energies and material geometry. Because of this situation it is relatively difficult to predict in advance which physical models are more likely. Hence a succession of physical models have been examined in order of increasing complexity.

3.2.2.1 Simple Desorption. This process is the evaporation of adsorbed molecules from surface sites with uniform energy. It can be shown[5] that the outgassing rate by this process, $\dot{Q}$, can be represented by

$$\dot{Q} = \frac{C_o}{\tau} \exp(-t/\tau) \text{ gm/cm}^2\text{/sec} \qquad (3)$$

where

$$\tau \sim 1.6 \times 10^{-13} \exp(E_a/RT) \text{ secs} \qquad (4)$$

C_o is the initial of adsorbed gas surface concentration, gms/cm^2 and E_a is the activation energy for desorption. These equations are clearly similar in form to the empirical equations (1) and (2). However, the experimentally measured time constant, t_c, is very much larger than

5. de Boer, J. H., The Dynamical Character of Adsorption, Clarendon Press (Oxford), 1953, Chapters 3 and 4.

the theoretical time constant, τ. Consequently, the simple desorption model would predict a far too rapidly decaying rate.

3.2.2.2 Multi-Energied Desorption. This model is similar to simple desorption, except that the activation energy is allowed to vary with surface coverage. It has been widely reported in the literature that in many situations activation energy varies linearly with coverage. This situation can be expressed by the following expressions

$$E(\theta) = E_1 + (E_2 - E_1)\theta \tag{5}$$

$$\dot{Q}(\theta)d\theta = \frac{C_o\, d\theta}{\tau(\theta)} \cdot \exp\left(-t/\tau(\theta)\right) \tag{6}$$

$$\tau(\theta) = 1.6x.10^{-13}\exp\left(E(\theta)/RT\right) \tag{7}$$

$$\dot{Q}_T = \int_o^1 \dot{Q}(\theta)d\theta \tag{8}$$

Equation (5) expresses the linear variation of the activation energy, E, with normalized coverage distribution function θ between minimum and maximum energies of E_1 and E_2. Equation (6) is the desorption rate of molecules at time t from sites of activation energy $E(\theta)$, with initial surface concentration C_o gms/cm^2 and residence time $\tau(\theta)$. Equation (7) relates $\tau(\theta)$ to activation energy. Equation (8) states that the total outgassing rate, $\dot{Q}_T$, is the integral of $\dot{Q}(\theta)$ with respect to the distribution function. A good fit was obtained to the 25°C isotherm using C_o equal to 10^{-6} gms/cm^2, and E_1 and E_2 equal to 21750 and 24000 cals/mole, respectively. These energies are considered to be improbably high for physical adsorption, but could indicate weak chemisorption. However, when the model was used to predict the outgassing rate for the lower temperature isotherms the correct curve shapes were obtained, but the magnitude of the reduction in rate with temperature was far too great - by as much as three orders of magnitude for the -54°C case. This large change is due to the energy values being too high.

The model was modified to account for the possibility of surface mobility of adsorbed gas. As molecules are desorbed from the surface sites some high energy sites will become vacant before all the low energy sites have been emptied. It is conceivable that molecules still adsorbed in lower energy sites could migrate across the surface to these vacated higher energy sites. This effect would tend to reduce the outgassing rate and extend the process for given values of E_1 and E_2, and should therefore permit a curve fit to be obtained for the 25°C data with lower values for E_1 and E_2. This modification was made to the model and the new values obtained for E_1 and E_2 were 21,500 and 23,500 cals/mole, respectively. As expected, this model did predict a smaller reduction in outgas rate with lowered temperature than the previous model, but the difference was insignificantly small. Since no further simple reasonable modifications to the adsorption model were apparent it was concluded at this point that the outgassing process was not surface-force controlled.

3.2.2.3 Simple Diffusion. It is possible that the outgassing mechanism under study could be due to diffusion through the Mylar and the metallic film of molecules originating in the Mylar or to diffusion of molecules sorbed in the oxide film, as has been suggested by Dayton.[6] In either case, if the diffusion process has a uniform activation energy, and if the material through which the gas diffuses is an infinitive plane with constant thickness, 2L, the outgas rate is given by

$$\dot{Q} = \frac{\pi}{8} \frac{C_o L}{\tau} \sum_{m=o} \exp\left[-\frac{\pi^3}{64\tau} \cdot (2m+1)^2 t\right] \qquad (9)$$

6. Dayton, B. B., Outgassing Rate of Contaminated Metal Surfaces, Transactions of the Eighth National Vacuum Symposium, (1961), Pergaman Press, New York, (1962), pp 42-57.

where

$$\tau = \frac{\pi L^2}{16D} \tag{10}$$

Here C_o is the initial concentration of outgas species, gms/cm^3, and D is the diffusion constant, given by

$$D = D_o \exp\ (-E_d/RT)\ \ \text{cm}^2/\text{sec} \tag{11}$$

where D_o is a constant and E_d is the activation energy for diffusion. Equation (9) expresses an outgassing/time characteristic whose initial segment shows $\ell n\dot{Q} = (-\frac{1}{2}\ \ell n\ (\text{time}) + (\text{constant}))$ while for long evacuation times $\ell n\dot{Q} \sim (\text{time})^{-1}$. For simple diffusion, cooling the sample will reduce the outgassing rate and extend the duration of the $(-\frac{1}{2})$ power dependency regime, but under no circumstances can the characteristic have a slope of less than $(-\frac{1}{2})$. It is clear from Figure 4 that as the temperature is reduced the slope of the data approches zero and hence they cannot possibly be representable by a simple diffusion model.

3.2.2.4 Complex Diffusion. The foregoing process of elimination has led the authors to believe that the correct model is some form of the diffusion equation (9), modified to include some combination of nonuniform activation energy, and/or nonuniform material thickness. Three possible scenarios exist: diffusion of gas originating only in the Mylar with and without significant diffusion resistance from the metallic film, and diffusion of gas originating only in the metallic oxide film micropore structure (Dayton's model). Analysis of these situation is in progress at the time of writing. The basic approach being used is to rewrite equations (9) and (11) to include a variable value of E_d, either as a function of location, or of the instantaneous value of local concentration. Variations in the predicted outgassing rate can be effected by manipulating the form of the variation of E_d, or by varying D_o. It has been

found that such manipulations do permit curves to be obtained with the same slopes as the data and also having the correct relationship between isotherms although some difficulty has been encountered in predicting the correct absolute value of outgassing rate. It has been concluded that the extent of the manipulations of E_d and D_o required to obtain this qualitative agreement excludes the possibility of the outgassing originating only from the oxide film, and hence excludes the Dayton model. Work will now be concentrated on further exploring the possibilities of the single medium model - Mylar alone - as well as extending the model to include two media - Mylar and aluminum film - in series.

4.0 CONCLUSIONS

The work performed to date has led to two very clear cut conclusions. On the one hand the QCM-based apparatus has proven to be very accurate, reproducible, reliable in generation of outgassing data and economical in personnel time to operate. It has been in continuous operation for six months without failure. On the other hand, only limited success has been achieved so far in identifying a viable analytical model for predicting the outgassing isotherms of even one portion of the data for one material. Although the effort involved is, indeed, generating insight into fundamental mechanisms, there is a little doubt that, given the excellent performance of the experimental apparatus, the most economical method of determining the dependence of outgassing behavior of a material on time and temperature is still to measure it directly.

5.0 ACKNOWLEDGEMENTS

This work was performed as part of a Lockheed Independent Research Program.

6.0 REFERENCES

1. Keller, C. W., High-Performance Thermal Protection Systems," Rept. LMSC A-964947, Dec. 1969, Lockheed Missiles & Space Co., Sunnyvale, Ca., pp 4.1 - 4.26.

2. Glassford, A. P. M., Outgassing Behavior of Multilayer Insulation Materials, J. Spacecraft and Rockets, Vol. 7, No. 12, Dec. 1970, pp 1464-1468.
3. Parmley, R. T., Smith, F. J., Glassford, A. P. M., Coleman, J., and Stevenson, D. R., Effect of Environment on Insulation Materials - Vols. 1 and 2, NASA-CR 120978 and 120979 (1973), Final Report, Contract NAS 3-14342, Lockheed Missiles & Space Co., Inc.
4. Glassford, A. P. M., Analysis of the Accuracy of a Commercial Quartz Crystal Microbalance, Progress in Astronautics and Aeronautics, Volume 56, Allie M. Smith, Ed., American Institute of Aeronautics and Astronautics, New York, (1977).
5. de Boer, J. H., The Dynamical Character of Adsorption, Clarendon Press (Oxford), 1953, Chapters 3 and 4.
6. Dayton, B. B., Outgassing Rate of Contaminated Metal Surfaces, Transactions of the Eighth National Vacuum Symposium, (1961), Pergaman Press, New York, (1962), pp 42-57.